# Harmonics as an alternative method for measuring I-0 during x-ray absorption spectroscopy experiments at laboratory scale

Bes, Rene

2021-04-01

Bes , R , Takala , S & Huotari , S 2021 , ' Harmonics as an alternative method for measuring I-0 during x-ray absorption spectroscopy experiments at laboratory scale ' , Review of Scientific Instruments , vol. 92 , no. 4 , 043106 . https://doi.org/10.1063/5.0046893

http://hdl.handle.net/10138/342265
https://doi.org/10.1063/5.0046893

unspecified
publishedVersion

Review of Scientific Instruments

# Harmonics as an alternative method for measuring $I_0$ during x-ray absorption spectroscopy experiments at laboratory scale

Cite as: Rev. Sci. Instrum. **92**, 043106 (2021); https://doi.org/10.1063/5.0046893
Submitted: 08 February 2021 . Accepted: 05 April 2021 . Published Online: 21 April 2021

René Bes, Saara Takala, and Simo Huotari

Review of Scientific Instruments ARTICLE scitation.org/journal/rsi

# Harmonics as an alternative method for measuring $I_0$ during x-ray absorption spectroscopy experiments at laboratory scale

Cite as: Rev. Sci. Instrum. 92, 043106 (2021); doi: 10.1063/5.0046893
Submitted: 8 February 2021 • Accepted: 5 April 2021 •
Published Online: 21 April 2021



René Bes,[1,2,a)] Saara Takala,[1] and Simo Huotari[1]

## AFFILIATIONS

[1] Department of Physics, University of Helsinki, P.O. Box 64, FI-00014 Helsinki, Finland
[2] Helsinki Institute of Physics, P.O. Box 64, FI-00014 Helsinki, Finland

[a)] **Author to whom correspondence should be addressed:** rene.bes@helsinki.fi

## ABSTRACT

In the recent years, the advent of an efficient and compact laboratory-scale spectrometer for x-ray absorption spectroscopy experiments has been extensively reported in the literature. Such modern instruments offer the advantage to routinely use x-ray absorption spectroscopy on systematic studies, which is usually unconceivable at synchrotron radiation source facilities due to often limited time access. However, one limiting factor is the fact that due to laboratory x-ray source brightness compared to a synchrotron, two separate measures of the incoming and transmitted x-ray intensities, i.e., the so-called $I_0$ and $I_1$, respectively, are usually required. Herein, we introduce and discuss an alternative approach for measuring $I_0$ and $I_1$ simultaneously. Based on the usage of harmonics arising naturally from the use of monochromator crystals, the reliability and robustness of our proposed approach is demonstrated through experiments at the Co $K$-edge measured using Co metal foil and at the Nd $L_3$-edge measured in $Nd_2O_3$.



## I. INTRODUCTION

X-ray absorption spectroscopy (XAS) is a non-destructive method for probing the element-specific electronic and local atomic structures of materials. Since decades, XAS experiments have been mainly performed at synchrotron facilities because of their extreme high brilliance and ability to provide monochromatic and most importantly energy-tunable x rays with a narrow bandpass. An alternative to synchrotron based XAS facilities is based on laboratory-scale sources (standard x-ray tubes) and wavelength-dispersive monochromator crystal optics that use the Bremsstrahlung produced by the x-ray tube. Such laboratory-scale devices have been regularly reported since the discovery of x rays until today,[1–25] have attracted more attention in the past few years, and are even commercially available. The aim of an XAS experiment is to measure the photoabsorption coefficient $\mu(E)$ as a function x-ray photon energy $E$ with a high resolution around a specific element's absorption edge. The study of the absorption coefficient is commonly divided into two separate applications: x-ray absorption near the edge structure (XANES) and the extended x-ray absorption fine structure (EXAFS), both yielding information on the local chemical neighborhood of the absorbing element. There are various detection modalities for XAS, including direct x-ray transmission measurements, and different types of secondary yield methods such as total fluorescence yield (TFY) and total electron yield (TEY). In the transmission mode, one notes that the attenuation of x rays in matter at a given energy $E$ is dictated by Beer–Lambert's law, which states that the x-ray flux $I(E)$ transmitted through a sample with thickness $d$ is related to the incident x-ray flux $I_0(E)$ and the photoabsorption cross section $\mu(E)$ as

$$I(E) = I_0(E)e^{-\mu(E)d}. \quad (1)$$

At a synchrotron XAS facility, $I(E)$ and $I_0(E)$ are measured simultaneously with, e.g., ionization chambers. In laboratory-based instruments, the $I(E)$ and $I_0(E)$ spectra are usually collected separately, i.e., performing the experiment sequentially with and without a sample. This strategy assumes inherently that the incident flux $I_0$ is invariant with time. This is generally justified because the radiation spectrum and flux of modern x-ray tubes are very stable. However, such an approach, nevertheless, suffers from the fact that it requires

two separate measurements instead of one, which increases the overall time required for the data collection as well as the risk that any $I_0$ instability remains unnoted or wrongly attributed to $I$. In addition, if the sample is enclosed in a complex environment such as an operando electrochemical or catalytic reactor or otherwise has to be enclosed in a nontrivial cell (such as radioactive samples), removal of the sample and its environment for the measurement of $I_0$ may have unknown effects on the spectrum. Then, it may be difficult if not impossible to obtain reliable data with the two-phase measurement strategy (with and without a sample). In our previous study at the U $L_3$-edge using the laboratory-scale XAS apparatus developed at the University of Helsinki[19] and equipped with one Ge(1 1 1) analyzer crystal,[26] it was found that the sample double encapsulation into Kapton and polyethylene affected the overall detected signal. Despite the use of slits to limit beam divergence and shielding to reduce background detection, those unexpected effects were certainly the consequence of the detection of a background signal, which was previously cut or even scattered by the sample encapsulation. To overcome this issue, one may think about measuring $I_0$ in the presence of an empty sample encapsulation. Whenever this solution is impossible or unpractical, having alternatives to simultaneously measure the incoming and the transmitted x-ray beam is of high interest for users of laboratory-scale XAS spectrometers. In our previous study,[26] we found that the use of the higher- or lower-level harmonics reflected by the monochromator crystal constitutes a good alternative to measure $I_0$ or to keep track of any instability that may occur during the $I$ collection step. Therefore, in this paper, we describe in detail the proposed method, its principle, and its limitations. Measurement at the Co $K$-edge and Nd $L_3$-edge was performed by means of Ge(1 1 1) and Si(1 1 1) monochromator crystals, respectively. The corresponding results are given as practical examples.

## II. PRINCIPLE OF USING HARMONIC AS $I_0$

### A. General idea behind the method

The wavelength-dispersive optics uses Bragg's law $n\lambda = 2d_{hkl}\sin\theta$, where $n$ is the harmonic order of the reflection, $\lambda$ is the wavelength of the x-ray light, $d$ is the lattice spacing of the monochromator crystal, and $\theta$ is the Bragg angle. The intensity of the reflection harmonic is given by the structure factor $F_{n(hkl)}$, where the notation $n(hkl)$ refers to the Miller indices of the $n$th harmonic of the lowest-order allowed reflection $hkl$ of the crystal orientation. For instance, $n = 3$ and $h = k = l = 1$ correspond to the (3 3 3) reflection. $F_{n(hkl)}$ can be zero in the case of a forbidden reflection. At this stage, it is natural to convert the energy in $I(E)$ and $I_0(E)$ to the corresponding quantities in the Bragg-angle space, $I(\theta)$ and $I_0(\theta)$. The total intensity $I(\theta) = \sum_n I^{(n)}(\theta)$, where $I^{(n)}(\theta)$ is the intensity of the $n$th order harmonic arriving at the detector; the same applies to $I_0$, i.e., $I_0(\theta) = \sum_n I_0^{(n)}(\theta)$. To separate the different contributions of the harmonics, it is necessary to be able to discriminate them, e.g., with an energy-dispersive detector. Let us assume that the spectrometer's Bragg-angle range is such that the energy range across the interesting element's absorption edge is covered by the $n$th harmonic, but at the same time, also the $m$th harmonic ($m \neq n$) is measured by using an energy-dispersive detector with its intensity recorded. From Eq. (1) with the above nomenclature, the photoabsorption cross section can be written as

$$\begin{aligned}\mu(\theta) &= -\ln\frac{I^{(n)}(\theta)}{I_0^{(n)}(\theta)} = -\ln\left[\frac{I^{(n)}(\theta)}{I^{(m)}(\theta)}\frac{I^{(m)}(\theta)}{I_0^{(n)}(\theta)}\right]\\ &= -\ln\left[\frac{I^{(n)}(\theta)}{I^{(m)}(\theta)}\right] - \ln\left[\frac{I^{(m)}(\theta)}{I_0^{(n)}(\theta)}\right]\\ &= -\ln[A(\theta)] - \ln[B(\theta)]. \qquad (2)\end{aligned}$$

When investigating Eq. (2), an interesting finding can be made. Recall that far from absorption edges, $I^{(m)}(\theta)$ is expected to follow the so-called Victoreen law[27] and approximately depends on energy as $aE^{-3} + bE^{-4}$, with $a$ and $b$ being constants. Since also the x-ray tube's Bremsstrahlung spectral shape is a very broad function, in the typical range of XANES spectra and possibly even in the EXAFS range, $B(\theta)$ may be approximated as a monotonic function and in most cases linear. A theoretical example demonstrating such a linear behavior for $B(\theta)$ is given in Fig. 1 for an Ag x-ray tube at 25 kV accelerating voltage, a Si(1 1 1) monochromator crystal, and

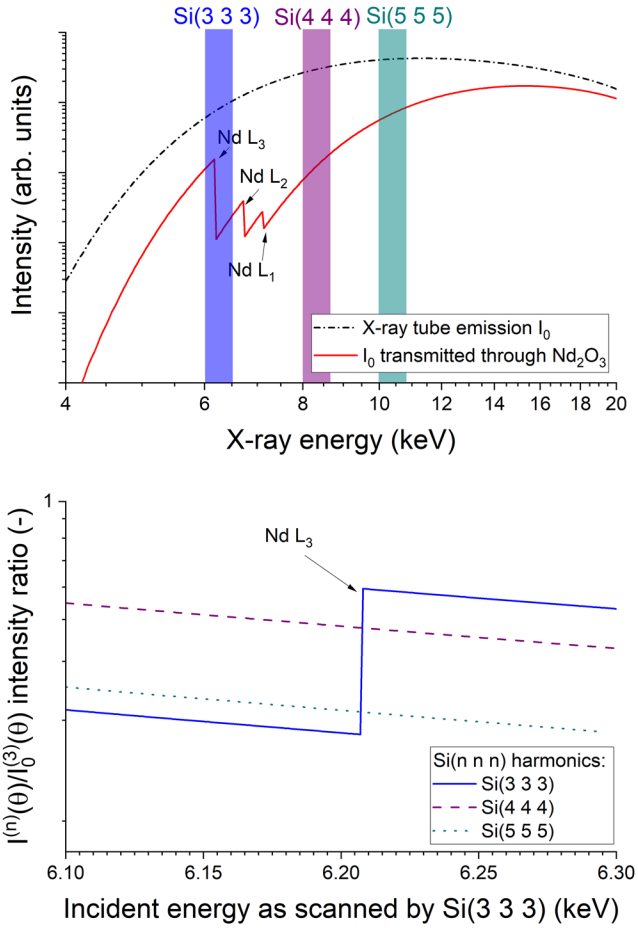


**FIG. 1.** Theoretical behavior of both $I_0$ and I for a 25 kV Ag x-ray tube, a Si(1 1 1) monochromator crystal, and a $Nd_2O_3$ transmission sample. The behavior of $B(\theta)$ as a function of the harmonic order along a typical Nd $L_3$-edge XANES energy range is also given.

a $Nd_2O_3$ transmission sample. The corresponding x-ray transmission values were obtained using the total x-ray attenuation cross section with coherent scattering available from the NIST Photon Cross Sections Database XCOM.[28]

The linear behavior of $B(\theta)$ means that it effectively acts as a separable background that can be subtracted. Since a linear background subtraction to $\mu(E)$ is usually made in any case in order to subtract the contributions of absorption of other electrons with lower binding energy as well as to scattering, it may be practically disregarded. The novelty in this finding is now that the interesting function $A(\theta) = I^{(n)}(\theta)/I^{(m)}(\theta)$ can be obtained with a single measurement. Namely, both $I^{(n)}(\theta)$ and $I^{(m)}(\theta)$ can be obtained simultaneously with an energy-dispersive detector if its energy resolution is high enough for the separation of the harmonics. This helps greatly to overcome challenges of experiments where either $I_0(E)$ or $\mu(E)$ may vary as a function of time during the course of the measurement of $I(E)$ or when some complex sample geometry simply prevents from measuring $I^{(n)}(\theta)$ and $I_0^{(n)}(\theta)$ separately in a reliable manner. In addition, the harmonic signal can also be seen as an alternative way to distinguish between possible $I_0$ time instabilities, when collecting $I$, from real changes in $I$ features arising from beam damage on highly sensitive samples or during, e.g., *in situ* catalysis experiments.

In order for $B(\theta)$ to be approximately linear in a XANES range, the absence of sharp spectral features such as x-ray tube emission lines, fluorescence lines, or other x-ray absorption edges is required within the Bragg angle of interest and at least for one of the available harmonics. This constitutes the major limitation of the proposed approach because it cannot always be achieved, especially when considering the presence of fluorescence lines in the x-ray tube overall emission spectra. To ensure that there is no spectral feature in the harmonic used as an $I_0$ measurement alternative, a quick measurement beforehand with and without the sample is still necessary to determine the behavior of $B(\theta)$, to verify that there are no unexpected features, and that $B(\theta)$ is, indeed, linear.

### B. Non-constant behavior correction

As regularly observed during our experiments, in the absence of any spectral features along the energy range of interest, $B(\theta)$ behaves in the best case linearly as a function of energy as a consequence of the Bremsstrahlung shape (see, e.g., Fig. 1). Then, applying the harmonic method would subsequently affect the deduced absorption coefficient $\mu(E)$ in a similar way. For the linear behavior case, the impact on $\mu(E)$ can be simply corrected by the background subtraction usually performed using a pre-edge linear function in standard XAS data analysis. In other cases, the non-constant behavior of $B(\theta)$ can be evaluated by standard fitting methods to obtain a smooth, fitted, function $B^f(\theta)$. Then, one may correct $\mu(E)$ by replacing the second term in Eq. (2), which becomes

$$\mu(\theta) = -ln\left(\frac{I^{(n)}(\theta) \times B^f(\theta)}{I^{(m)}(\theta)}\right). \quad (3)$$

Such a correction is theoretically applicable for any type of function $B^f(\theta)$, as long as a correct evaluation of it has been made, which is not always an easy task when behaving far from linearity unless one has collected enough statistics to ensure low uncertainties. Moreover, detector response could be in some cases affected by the intensity differences with and without the sample, leading to incorrect evaluation of $B^f(\theta)$. Correction on a case to case basis is, thus, highly recommended.

## III. PRACTICAL EXAMPLES

In the following parts, we discuss the application of the harmonic as an $I_0$ approach to the measurements of Co $K$-edge and Nd $L_3$-edge XAS spectra.

### A. Sample preparation

The Co $K$-edge spectra were collected using 10 $\mu$m thick Co metallic foil. The Nd $L_3$-edge XAS spectra were collected using a $Nd_2O_3$ transmission pellet, prepared by mixing ~7 mg of pure $Nd_2O_3$ powder (purity about 99.999%) supplied by Alfa Aesar (Karlsruhe, Germany) with 200 mg boron nitride powder and pressed to a thickness of 0.5 mm and 12 mm diameter. This pellet was then confined between 8 $\mu$m thick Kapton foils to avoid air contact and ensure easy handling.

### B. Experimental conditions

The detailed description of the Johann-type laboratory-scale x-ray absorption spectrometer used in this study has been discussed elsewhere.[19] The x-ray source was a fine-focus Ag anode 1.5 kW x-ray tube (Seifert/XRD Eigenmann) with a 0.4 × 0.8 $mm^2$ effective source size (H × V). The accelerating potentials were fixed to 15 and 10 kV for the Co $K$-edge (7.709 keV) and the Nd $L_3$-edge (6.208 keV), respectively. A 4 mA electron current was kept in both cases.

The focusing and monochromatization of polychromatic x-rays were achieved by means of strip-bent Si(1 1 1) and Ge(1 1 1) spherically bent analyzer crystals. The former was provided by the European synchrotron radiation facility (ESRF) crystal analyzer laboratory,[18] while the latter was provided by XRS TECH LLC. Both crystals have a bending radius of 500 mm and a surface diameter of 100 mm. The Co $K$-edge XANES spectra were collected using the Ge(4 4 4) reflection, from 7.65 to 7.95 keV. The Nd $L_3$-edge XANES spectra were collected using the Si(3 3 3) reflection, from 6.15 to 6.37 keV.

Samples were positioned in transmission mode in front of the x-ray source.

A Si detector (Amptek XR-100CR) with an active surface of ~3 mm in diameter was used. The good energy resolution of the Si solid-state detector allowed us to well discriminate between different x-ray harmonics, as shown in Fig. 2.

In both cases, a quick glance at the detected signal demonstrated harmonics being well separated by the detector energy resolution. The observed harmonics correspond to what one may expect for an x-ray tube accelerating voltage of 10 and 15 kV coupled to Si(1 1 1) and Ge(1 1 1) analyzer crystals, respectively. No additional peaks are observed, meaning that only x rays reflected by the monochromator crystal are detected. However, it has to be mentioned that in the case of Si(1 1 1), the x-ray tube accelerating potential was limited to 10 kV to avoid W $L_3$-edge (10.207 keV) excitation and subsequent detector saturation, W being a natural contamination of our x-ray tube during aging. Indeed, within the Bragg-angle range of interest for the Nd $L_3$-edge, the Si(4 4 4) energy range overlaps W $L_3M_4$ and

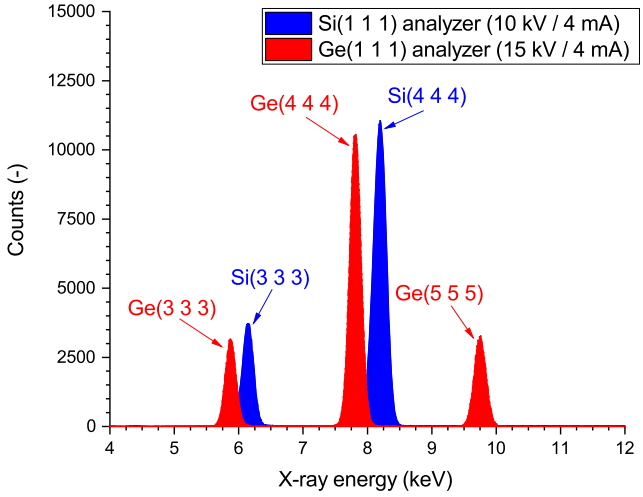


**FIG. 2.** Harmonics detected when using the laboratory-scale XAS spectrometer equipped with Si(1 1 1) and Ge(1 1 1) analyzer crystals. The x-ray tube accelerating potentials were 10 and 15 kV, respectively. The electron current was 4 mA in both cases.

$L_3M_5$ emission lines at 8.3976 and 8.3352 keV, respectively. Arising from the excitation of the W $L_3$-edge, those W signals, when present, limit the Nd $L_3$-edge XANES spectra to a maximum energy of about 6.29 keV.

In the case of the Co *K*-edge, the W emission lines do not overlap the energy ranges covered by Ge(4 4 4) or Ge(3 3 3). Thus, the accelerating voltage was increased to 15 kV to get the maximum of the Bremsstrahlung closer to the Co *K*-edge energy. In this case, the Ge(5 5 5) harmonic is also observed in the detected signal, as seen in Fig. 2. Covering energies ranging from 9.56 to 9.94 keV, W fluorescence lines such as $L_3N_1$, $L_2M_4$, and $L_1M_3$ are expected to be observed in the Ge(5 5 5) signal. Their branching ratio is, however, rather small.

## C. Raw XANES spectra

The behavior of $B(\theta)$ for both Co *K*-edge and Nd $L_3$-edge was determined using available harmonics compared to the standard $I_0$ measurement, i.e., the Si(3 3 3) and Ge(4 4 4) harmonics without the sample, respectively. Such behavior is presented in Fig. 3 as well as the resulting raw XANES spectra.

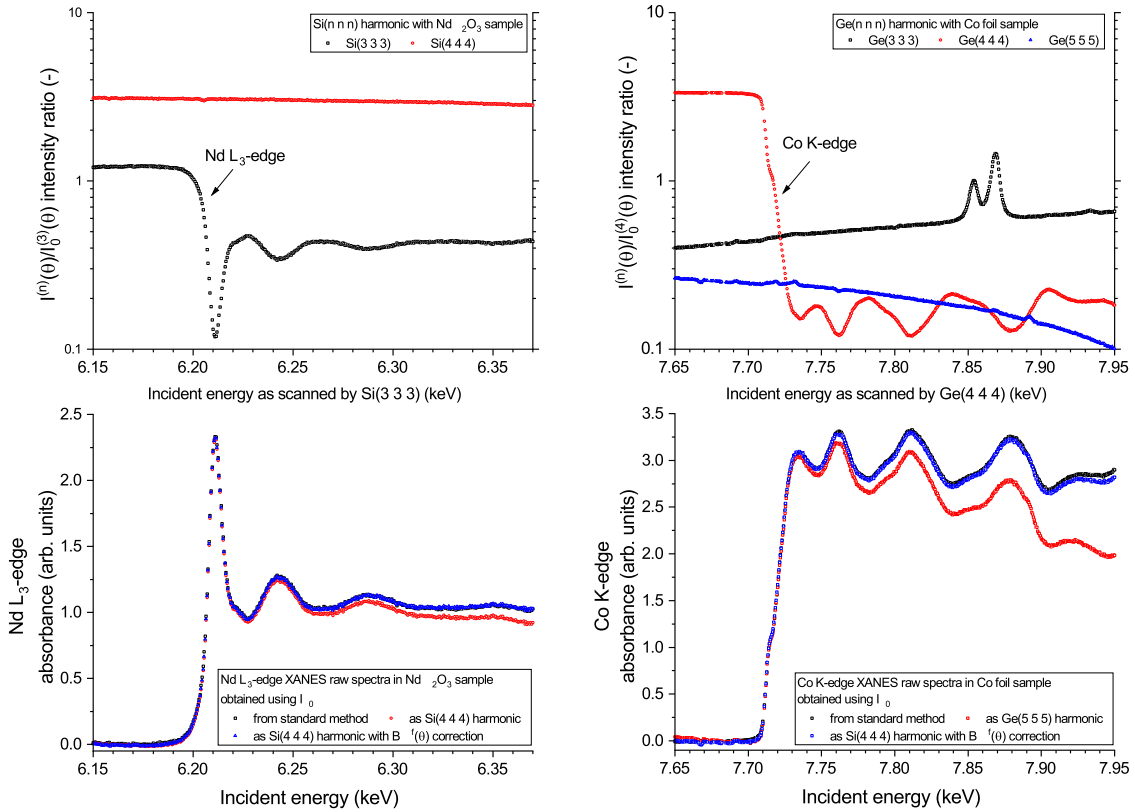


**FIG. 3.** Behavior of $B(\theta)$ as a function of the harmonic order from Ge(1 1 1) and Si(1 1 1) analyzer crystals in the case of the Co *K*-edge and Nd $L_3$-edge, respectively. A comparison of the resulting Co *K*-edge and Nd $L_3$-edge XANES raw spectra is also provided with and without non-constant behavior correction.

#### 1. Nd $L_3$-edge

$B(\theta)$ behaves almost linearly and smoothly along the scanned energy range for Si(4 4 4). The deduced XANES raw spectra look very similar and show the well-known characteristic shape of the Nd $L_3$-edge in $Nd_2O_3$. Deviation of the harmonic obtained spectra from the spectra obtained using the standard approach arises when increasing energy. The fact that $B(\theta)$ is not constant but behaves roughly linearly with energy in the XANES range leads to this linear distortion when applying the harmonic as the $I_0$ approach compared to the standard $I_0$ measurement. As discussed earlier, this could be easily corrected by introducing a function of energy $B^f(\theta)$ deduced from a linear fit of $B(\theta)$. We applied this correction method, and the resulting spectrum is also shown in Fig. 3. The correction applied following Eq. (3) perfectly compensates the observed distortion. Indeed, both standard and harmonic corrected spectra are well superimposed all along the energy range and within statistical noise, meaning that the non-linear correction does not introduce additional distortions or features.

#### 2. Co K-edge

Contrary to what was observed for the Nd $L_3$-edge, the $B(\theta)$ shapes and behaviors are not ideal for the proposed method. Being almost linear and smooth for Ge(3 3 3), $B(\theta)$ behavior shows two peaks that were unexpected. Those peaks correspond to Mn $KL_2$ (5.888 keV) and $KL_3$ (5.899 keV) and *de facto* exclude Ge(3 3 3) as a reliable harmonic for measuring $I_0$. The origin of this extra fluorescence signal was an unexpected Mn pollution of the x-ray tube used in this experiment.

Among the available harmonics, only Ge(5 5 5) remains available. For Ge(5 5 5), $B(\theta)$ behaves almost smoothly, but it is clearly not linear in its high energy part. The observed curvature is the consequence of the Bremsstrahlung shape and its intensity decreasing rapidly in the vicinity of the x-ray tube accelerating voltage, fixed here to 15 kV. This behavior explains the significant deviation of the harmonic obtained spectra from the spectra obtained using the standard approach when increasing energy. Using a correction $B^f(\theta)$ deduced from a third-order polynomial fit of $B(\theta)$ partially corrects the distortion, both corrected and standard spectra superimposing well. The distortion is finally well compensated during the usual XAS data analysis including EXAFS extraction as demonstrated later.

### D. EXAFS spectra

The ATHENA software[29] was used for normalizing XANES spectra and extracting the EXAFS spectra from the raw absorption data obtained using $I_0$ from the standard method and as Si(4 4 4) harmonic, without any preliminary applied correction. The energy threshold $E_0$ value was chosen as the first knot of the first derivative relatively to the incident energy in each spectrum. Pre-edge background removal and post-edge normalization were achieved using linear functions, keeping identical parameters for all spectra. The EXAFS data fitting process has been performed with a k-weight value of 2 by using the ARTEMIS software.[29] Experimental EXAFS spectra were Fourier transformed using a Hanning window over the full k range available, i.e., [2.5, 6.0] and [2.0, 7.0] $Å^{-1}$ for the Nd $L_3$-edge and Co *K*-edge, respectively. Given the short k range, only the first coordination shell was considered for fitting. Phases and amplitudes of the interatomic scattering paths were calculated with the *ab initio* code FEFF8.40. The shift in threshold energy $\Delta E_0$ and the amplitude reduction factor $S_0^2$ were varied as global parameters for each edge.

#### 1. Nd $L_3$-edge

The $B^f(\theta)$ correction introduced earlier was almost linear and, therefore, did not require to be corrected before standard XAS analysis. The results are shown in Fig. 4.

As demonstrated in Fig. 4, both spectra are perfectly superimposed, in both XANES and EXAFS. As expected, the only slight differences visible come from statistical differences.

$Nd_2O_3$ crystallizes in the trigonal centrosymmetric space group $P\bar{3}m1$,[30] having a = b = 3.83(1) Å, c = 6.00(3) Å, $\alpha = \beta = 90°$, and $\gamma = 120°$. The environment surrounding the Nd sites consists of 7 oxygen ions, three of them situated at 2.66 Å, three others at 2.30 Å, and the last one at 2.41 Å. EXAFS fitting of the first coordination shell was realized using a 6 Å cluster of this $P\bar{3}m1$ crystal structure. However, only one Nd–O single-scattering path was included to fit the first shell structural parameters from EXAFS spectra, following the Fourier transform peak separation resolution of 0.45 Å as given by the Rayleigh criterion.

The EXAFS fit was equally successful for both spectra obtained using the standard and uncorrected harmonic approaches. No significant differences are observed when comparing the extracted structural parameters, as reported in Table I, demonstrating the reliability of the proposed harmonic alternative.

#### 2. Co K-edge

The $B^f(\theta)$ correction introduced earlier was a third-order polynomial. As third-order polynomial functions are often used for post-edge normalization in standard XAS analysis, we only considered the uncorrected harmonic spectrum in the following. The results of the XAS normalization and EXAFS signal extraction are shown in Fig. 5.

As demonstrated in Fig. 5, both spectra are well superimposed in both XANES and EXAFS, where only slight differences due to statistical differences are visible.

Cobalt crystallizes in the cubic space group $Fm\bar{3}m$, having a = b = c = 3.42 Å and $\alpha = \beta = \gamma = 90°$. The Co first shell coordination number is 12 cobalt atoms, all of them situated at 2.418 Å. EXAFS fitting of the first coordination shell was realized using a 5 Å cluster of this $Fm\bar{3}m$ crystal structure.

The EXAFS fit was equally successful for both spectra obtained using the standard and uncorrected harmonic approaches. No significant differences are observed when comparing the extracted structural parameters, as reported in Table II.

Despite slight differences within the uncertainty errors, these results demonstrate the ability of the proposed alternative approach to replace time consuming $I_0$ measurement during XAS in transmission experiments using a laboratory-scale apparatus.

## IV. TIME-SAVING CONSIDERATIONS

As demonstrated, the harmonic-as-$I_0$ approach can replace the standard $I_0$ measurement and can, therefore, provide substantial time-saving. To evaluate the potential time benefit of the harmonic-as-$I_0$ approach, one has to consider two parameters: $N_s$ and $N_h$

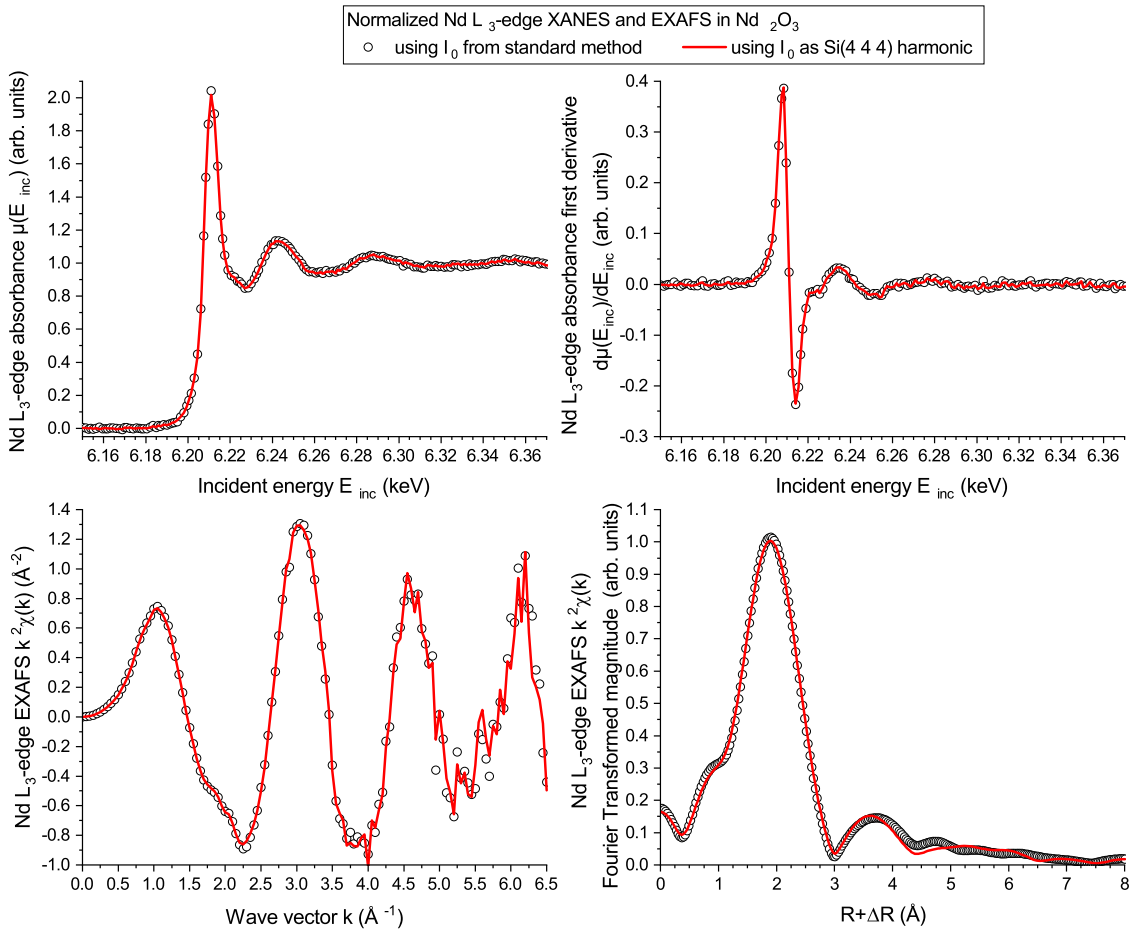


**FIG. 4.** Comparison between Nd $L_3$-edge normalized XANES spectra, their first derivative, the extracted $k^2\chi(k)$ EXAFS data, and their Fourier transformed magnitude, as obtained using $I_0$ from the standard approach and the harmonic alternative approach on the $Nd_2O_3$ sample.

defined as follows, keeping the same convention as that in Eq. (2):

$$N_s = \frac{I_0^{(n)}(\theta)}{I^{(n)}(\theta)},$$
$$N_h = \frac{I_0^{(n)}(\theta)}{I^{(m)}(\theta)} = \frac{1}{B(\theta)}. \quad (4)$$

**TABLE I.** EXAFS fitting deduced structural parameters for the O first coordination shell in the $Nd_2O_3$ sample. Both spectra from the standard and uncorrected harmonic approaches are compared. The shift in threshold energy $\Delta E_0$ was found equal to 5.6(4) eV. The coordination number was fixed to 7, while the amplitude reduction factor $S_0^2$ was fitted and found equal to 1.08(5). The fit correlation factor $R_{factor}$ in R-space is equal to 0.013 over the k range of (2.5; 6.0) $Å^{-1}$ and R range of (1.2; 3.0) Å.

| Spectrum | Distance (Å) | Debye–Waller ($Å^2$) |
|---|---|---|
| Standard $I_0$ | 2.535(10) | 12(3) $10^{-3}$ |
| Si(4 4 4) as $I_0$ | 2.534(8) | 12(2) $10^{-3}$ |

$N_h$ refers to the number of spectra needed for the harmonic-as-$I_0$ to reach similar statistics as obtained by one $I_0$ measurement. Similarly, $N_s$ is the required number of spectra with the sample. Indeed, independent of the $I_0$ evaluation method, a minimum of $N_s$ spectra is always measured, and this number usually represents the main time limiting factor due to the nature of the absorption process. Therefore, using the standard $I_0$ method requires to collect $(N_s + 1)$ spectra, while using the harmonic-as-$I_0$ method requires at least $N_s$ spectra up to a maximum of $N_h$ spectra when $N_h > N_s$. Consequently, the harmonic-as-$I_0$ approach is time beneficial whenever $N_h$ is lower than $(N_s + 1)$ and time detrimental otherwise.

Following those considerations, one can expect a maximum time benefit $t_{benefit}$ expressed in % as follows:

$$t_{benefit} = \frac{100}{N_s + 1}. \quad (5)$$

When thinking of $N_s$, the natural way of defining it is by means of the Beer–Lambert law, given that the x-ray tube current is kept

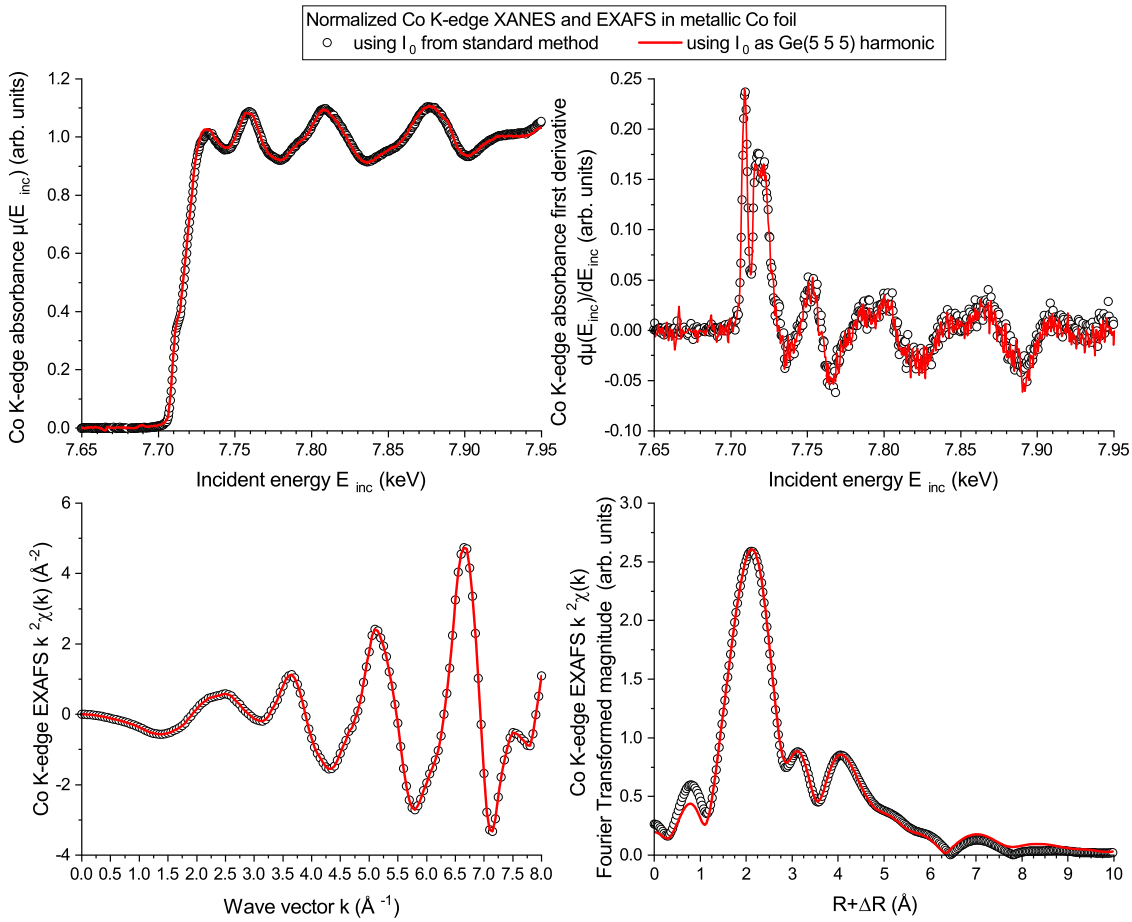


**FIG. 5.** Comparison between Co *K*-edge normalized XANES spectra, their first derivative, the extracted $k^2\chi(k)$ EXAFS data, and their Fourier transformed magnitude, as obtained using $I_0$ from the standard approach and the harmonic alternative approach on the Co foil sample.

identical for both $I_0$ and I count rate evaluations. For typical samples with the absorption length between 2 and 3, $N_s$ is, for instance, expected in the range of 7 to 20 spectra, giving $t_{benefit}$ in the range of 5%–15%. This was, for example, the case of the Co K-edge and Nd $L_3$-edge described in this paper. The measured time benefits were found around 15% of the total experiment duration, i.e., about 3–4 h per day.

**TABLE II.** EXAFS fitting deduced structural parameters for the Co first coordination shell in the metallic Co foil sample. Both spectra from the standard and uncorrected harmonic approaches are compared. The shift in threshold energy $\Delta E_0$ was found equal to 3.6(5) eV. The coordination number was fixed to 12, while the amplitude reduction factor $S_0^2$ was fitted and found equal to 0.79(4). The fit correlation factor $R_{factor}$ in R-space is equal to 0.019 over the k range of (2.0; 7.0) $Å^{-1}$ and R range of (1.2; 3.0) Å.

| Spectrum | Distance (Å) | Debye–Waller ($Å^2$) |
|---|---|---|
| Standard $I_0$ | 2.442(5) | 5.9(8) $10^{-3}$ |
| Ge(5 5 5) as $I_0$ | 2.444(9) | 5.4(9) $10^{-3}$ |

Quite often, the x-ray tube current is not chosen on the basis of $I_0$ count rate, but on the I count rate, in order to have the highest achievable count rate when measuring the sample without detector saturation. Then, one has to vary the source current down or insert attenuators for $I_0$ measurement to avoid subsequent detector saturation. Values below 7 are then allowed for $N_s$, giving maximum time benefits above 15%. However, varying the source current must be restricted to x-ray sources for which a strict proportionality relationship in energy spectra is expected when changing their current, at least within the energy ranges of interest. Similar care has to be taken when using attenuators. Such an attenuator approach was used, for example, during the U $L_3$-edge experiments described in Ref. 26. A substantial time benefit of 50%, i.e., 12 h per day of experiment, was observed thanks to the high intensity of the harmonic used as $I_0$. In this case, the limiting factor was actually the time needed for the I measurement itself.

## V. CONCLUSION

In this work, we have introduced an alternative approach for measuring $I_0$ during x-ray absorption spectroscopy experiments in

transmission using a laboratory-scale spectrometer. The Co *K*-edge measured in Co metal foil and the Nd $L_3$-edge measured in $Nd_2O_3$ were discussed as practical examples. Based on the usage of harmonics arising naturally from the use of monochromator crystals, the "harmonics-as-$I_0$" approach demonstrated its reliability and robustness and will certainly be useful to anyone desiring saving time by not repeating the measurement without the sample to obtain $I_0$ at the laboratory. It could also be mandatory in certain specific cases such as sample holder effects, likely to be absent when measuring $I_0$ without the sample. The harmonic-as-$I_0$ approach is also a good solution to follow the stability of $I_0$ during a very long experiment (several weeks) such as during *in situ* catalysis experiments. Indeed, during this type of experiments, the behavior of spectral features observed when measuring the sample needs to be reliably linked to the change within the sample itself, and possible $I_0$ instabilities can be easily ruled out by using the harmonic as an indirect stability measurement. The proposed alternative then constitutes a perfectly adapted solution for many such situations.

## AUTHORS' CONTRIBUTIONS

R.B. proposed the harmonic approach. R.B. and S.H. conceived the experiments. R.B and S.T. conducted the experiments and analyzed the results. All authors reviewed the manuscript.

## ACKNOWLEDGMENTS

This work was supported by the Academy of Finland (Grant No. 1295696) and by the GAMMA project of the Helsinki Institute of Physics. We thank the Center for x-ray Spectroscopy for providing experiment time and support with the HelXAS spectrometer under Proposal Number 2020-0006.

## DATA AVAILABILITY

The data that support the findings of this study are available from the corresponding author upon reasonable request.

## REFERENCES

[1] G. S. Knapp, H. Chen, and T. E. Klippert, Rev. Sci. Instrum. **49**, 1658 (1978).
[2] G. G. Cohen, D. A. Fischer, J. Colbert, and N. J. Shevchik, Rev. Sci. Instrum. **51**, 273 (1980).
[3] P. Georgopoulos and G. S. Knapp, J. Appl. Crystallogr. **14**, 3 (1981).
[4] A. Williams, Rev. Sci. Instrum. **54**, 193 (1983).
[5] W. Thulke, R. Haensel, and P. Rabe, Rev. Sci. Instrum. **54**, 277 (1983).
[6] K. Tohji, Y. Udagawa, T. Kawasaki, and K. Masuda, Rev. Sci. Instrum. **54**, 1482 (1983).
[7] K. Tohji and Y. Udagawa, Physica B **158**, 332 (1989).
[8] P. Lecante, J. Jaud, A. Mosset, J. Galy, and A. Burian, Rev. Sci. Instrum. **65**, 845 (1994).
[9] R. Verbeni, M. Kocsis, S. Huotari, M. Krisch, G. Monaco, F. Sette, and G. Vanko, in *5th International Conference on Inelastic X-ray Scattering (IXS 2004)* [J. Phys. Chem. Solids **66**, 2299 (2005)].
[10] Y. N. Yuryev, H.-J. Lee, H.-M. Park, Y.-K. Cho, M.-K. Lee, and K. J. Pogrebitsky, Rev. Sci. Instrum. **78**, 025108 (2007).
[11] Y. N. Yuryev, H.-J. Lee, J.-H. Kim, Y.-K. Cho, M.-K. Lee, and K. J. Pogrebitsky, X-Ray Spectrom. **37**, 476 (2008).
[12] M. Szlachetko, M. Berset, J.-C. Dousse, J. Hoszowska, and J. Szlachetko, Rev. Sci. Instrum. **84**, 093104 (2013).
[13] G. T. Seidler, D. R. Mortensen, A. J. Remesnik, J. I. Pacold, N. A. Ball, N. Barry, M. Styczinski, and O. R. Hoidn, Rev. Sci. Instrum. **85**, 113906 (2014).
[14] C. Schlesiger, L. Anklamm, H. Stiel, W. Malzer, and B. Kanngießer, J. Anal. At. Spectrom. **30**, 1080 (2015).
[15] Z. Németh, J. Szlachetko, É. G. Bajnóczi, and G. Vankó, Rev. Sci. Instrum. **87**, 103105 (2016).
[16] G. Seidler, D. Mortensen, A. Ditter, N. Ball, and A. Remesnik, J. Phys.: Conf. Ser. **712**, 012015 (2016).
[17] D. R. Mortensen, G. T. Seidler, A. S. Ditter, and P. Glatzel, J. Phys.: Conf. Ser. **712**, 012036 (2016).
[18] M. Rovezzi, C. Lapras, A. Manceau, P. Glatzel, and R. Verbeni, Rev. Sci. Instrum. **88**, 013108 (2017).
[19] A.-P. Honkanen, S. Ollikkala, T. Ahopelto, A.-J. Kallio, M. Blomberg, and S. Huotari, Rev. Sci. Instrum. **90**, 033107 (2019).
[20] A. S. Ditter, E. P. Jahrman, L. R. Bradshaw, X. Xia, P. J. Pauzauskie, and G. T. Seidler, J. Synchrotron Radiat. **26**, 2086 (2019).
[21] E. P. Jahrman, W. M. Holden, A. S. Ditter, D. R. Mortensen, G. T. Seidler, T. T. Fister, S. A. Kozimor, L. F. J. Piper, J. Rana, N. C. Hyatt, and M. C. Stennett, Rev. Sci. Instrum. **90**, 024106 (2019).
[22] W. Błachucki, J. Czapla-Masztafiak, J. Sá, and J. Szlachetko, J. Anal. At. Spectrom. **34**, 1409 (2019).
[23] F. Zeeshan, J. Hoszowska, L. Loperetti-Tornay, and J.-C. Dousse, Rev. Sci. Instrum. **90**, 073105 (2019).
[24] E. S. Joseph, E. P. Jahrman, and G. T. Seidler, X-Ray Spectrom. **49**, 493 (2020).
[25] P. Zimmermann, S. Peredkov, P. M. Abdala, S. DeBeer, M. Tromp, C. Müller, and J. A. van Bokhoven, Coord. Chem. Rev. **423**, 213466 (2020).
[26] R. Bès, T. Ahopelto, A.-P. Honkanen, S. Huotari, G. Leinders, J. Pakarinen, and K. Kvashnina, J. Nucl. Mater. **507**, 50 (2018).
[27] J. A. Victoreen, J. Appl. Phys. **20**, 1141 (1949).
[28] M. Berger, J. Hubbell, S. Seltzer, J. Chang, J. Coursey, R. Sukumar, D. Zucker, and K. Olsen, "Xcom: Photon cross sections database," 2010, note: NIST Standard Reference Database 8 (XGAM).
[29] B. Ravel and M. Newville, J. Synchrotron Radiat. **12**, 537 (2005).
[30] J. B. Gruber, B. H. Justice, E. F. Westrum, Jr., and B. Zandi, J. Chem. Thermodyn. **34**, 457 (2002).